Applied Thermal Engineering 35 (2012) 177–184

Contents lists available at SciVerse ScienceDirect

Applied Thermal Engineering

journal homepage: www.elsevier.com/locate/apthermeng

Solution to the 1-D unsteady heat conduction equation with internal Joule heat generation for thermoelectric devices

A. Montecucco*, J.R. Buckle, A.R. Knox

School of Engineering, College of Science and Engineering, University of Glasgow, Rankine Building, Glasgow G12 8LT, UK

ARTICLE INFO

Article history:
Received 28 June 2011
Accepted 14 October 2011
Available online 25 October 2011

Keywords:
Thermoelectric
Heat transfer
Heat generation
Heat conduction
Transient solution
Joule heating
Peltier
Seebeck

ABSTRACT

Thermoelectric devices are semiconductor devices which are capable of either generating a voltage when placed in between a temperature gradient, exploiting the Seebeck effect, or producing a temperature gradient when powered by electricity, exploiting the Peltier effect. The devices are usually employed in environments with time-varying temperature differences and input/output powers. Therefore it becomes important to understand the behaviour of thermoelectric devices during thermal and electrical transients in order to properly simulate and design complex thermoelectric systems which also include power electronics and control systems.

The purpose of this paper is to provide the transient solution to the one-dimensional heat conduction equation with internal heat generation that describes the transfer and generation of heat throughout a thermoelectric device. The solution proposed can be included in a model in which the Peltier effect, the thermal masses and the electrical behaviour of the system are considered too; this would be of great benefit because it would allow accurate simulations of thermoelectric systems.

While the previous literature does not focus on the study of thermal transients in thermoelectric applications and usually considers constant the temperatures at the hot and cold sides, this paper proposes a dynamic exchange of heat through the hot and cold side, both in steady-state and transients. This paper also presents an analytical solution which is then computed by Matlab to simulate a physical experiment. Simulation results show excellent correlation with experimentally determined values, thus validating the solution.

1. Introduction

Current literature [1,2] considers thermoelectric (TE) systems under steady-state and when in equilibrium. Few papers [3–7] consider the simulation of thermal transients found in practical TE systems, or effects due to variation in the electrical system parameters. Actually most thermoelectric applications are subject to electro–thermal transients. In cooling applications for electronic devices [8] heat is generated depending on use, therefore a controller is usually employed and its design needs to take transients into account. In thermoelectric power generation temperatures are often changeable, especially in applications to the automotive field [9,10] or to stoves [11,12], where start-up and shut-down considerations are a major concern. These problems are yet not fully assessed in literature and industry.

The following part of this section focuses on TE generators (TEGs), but similar considerations can be applied to Peltier devices.

The operation of thermoelectric devices depends on five main effects: (1) thermal conduction; (2) internal Joule heating; (3) Seebeck effect; (4) Peltier effect and (5) Thomson phenomenon, which is here neglected because of small effect [1,2].

The thermal power input to the hot junction is given by

$$q_H = \frac{kA\Delta T}{L} + \alpha T_H I - \frac{1}{2}R_{\text{int}}I^2 \tag{1}$$

where k is the overall conduction coefficient, A is the area and L the thickness of the TEG, ΔT is the temperature gradient, α is the Seebeck coefficient, T_H is the temperature at the hot side, I is the current produced and R_{int} is the overall internal resistance of the device.

As explained in a paper by Ben-Yaakov and Lineykin [3], Eq. (1) is derived from the steady-state solution of the one-dimensional heat conduction equation for solids with internal energy generation, which is written as:

$$\frac{\partial^2 T}{\partial x^2} + \frac{\dot{g}}{k} = 0 \tag{2}$$

* Corresponding author.
E-mail address: andrea.montecucco@glasgow.ac.uk (A. Montecucco).

1359-4311/$ – see front matter © 2011 Elsevier Ltd. All rights reserved.
doi:10.1016/j.applthermaleng.2011.10.026

where $\dot{g}$ is the rate of heat internally generated per unit volume [W/m^3] while T and k have the same meaning as in Eq. (1).

Assuming constant temperatures at the hot and cold side as boundary conditions ($T(t,0) = T_H$; $T(t,L) = T_C$), Eq. (2) can be solved as:

$$T(x) = T_H - \frac{\dot{g}}{2k}x^2 + \frac{T_C - T_H + \frac{\dot{g}}{2k}L^2}{L}x \tag{3}$$

Combining this result to the equation of heat transfer $q = (-kA)\partial T/\partial x$, the expression for the heat flow through the hot side becomes

$$q_H = \frac{kA\Delta T}{L} - \frac{1}{2}R_{\text{int}}I^2 \tag{4}$$

Taking into account the Peltier heating or cooling effect at the junctions this equation becomes Eq. (1).

The solution for the cold side is similar; the two results show that the Joule heating in the bulk material is equally divided between the hot and cold sides. This steady-state characterisation of TE devices accurately describes the balance of powers in a system under steady-state. However it is not usable in a time-varying environment because it does not take time into consideration and because the boundary conditions used to solve Eq. (2) assume that the temperatures at the hot and cold sides are constant.

Test results from a paper by Chen L. *et al.* [4], which investigates the electrical response of TE devices to load transients, show that a common TE module has a very fast dynamic response, in the order of nano-seconds. This means that the direct energy conversion taking place in the practical TE systems can be considered instantaneous. Hence it does not influence the thermal dynamics, which are controlled only by the thermal elements, i.e. thermal capacities of the system.

The thermal time constants of TE devices are of higher orders of magnitude if compared to the electrical ones. This means that there are "spikes" in power and efficiency before the thermal time constants bring the device to steady-state operation. When the operating conditions change simultaneously with time, the effects of these transients are so important that both the heat sources and the electronics is affected. Therefore their impact on the entire system, besides the steady-state behaviour, is important. Depending on the power input to the hot side, the number of modules and the power output from the cold side, these thermal transients can last for quite long periods of time, in the range of tens of seconds. To carefully design the whole system in cases of frequent changes of operation conditions and during start-up and shut-down, it becomes necessary to model these thermal transients and dynamic characteristics.

In both papers by Chen M. *et al.* [5], as well as in [3], the transient term is included in the (SPICE) model as a parallel electrical capacitor, converting the thermal model into an equivalent electrical circuit, to take into account an additional time-related term due to the change in stored heat energy. Therefore, considering an infinitesimal element dx inside the TE module, as in Fig. 1, the heat flow increase from the inlet to the outlet of the element is

$$\mathrm{d}q = q(x + \mathrm{d}x) - q(x) = R_{\text{int}}I^2 + mC_m\frac{\mathrm{d}T}{\mathrm{d}t} \tag{5}$$

where m and C_m are the mass and the specific heat of the element. Θ is the thermal resistance of dx.

A commonly used approach is to divide the module into a grid of small elements like dx, each one taking into account the heat conduction, the Joule heating, the Peltier heating/cooling and the thermal mass; hence an accurate equivalent circuit is composed by a series of RC cells. Additionally, other parts of the TE system, like the ceramic plates and the heat sinks, need to be included as

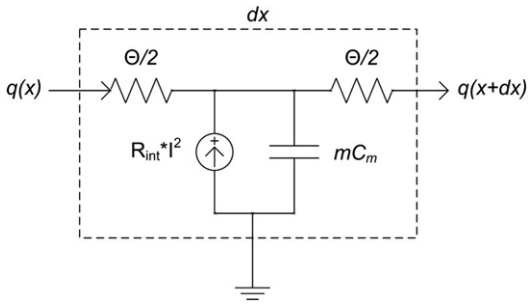

Fig. 1. Lumped equivalent circuit of the heat transfer in an infinitesimal volume dx inside the TE module [5].

thermal impedances. The accuracy of the simulation is related to the number of cells used, which needs to be tuned depending on if the thermal masses of these external elements are comparable, bigger or smaller than the one of the TE module. These kinds of models available for circuit simulators like SPICE and ANSYS do not offer a theoretical solution to the problem and are sometimes difficult to use, due to the division of the module in multiple elements, whose parameters are difficult to obtain from the data sheets of the manufacturers.

A more appropriate and more reliable approach would be to study these devices through the physical equations which describe their behaviour; among these, the most important is the heat equation. Alata, Naji and Al-Nimr [6,7] have already explored this possibility, but they used fixed temperatures as boundary conditions at the two sides of the TE module, assuming that those temperatures are not varying even if there is an exchange of heat through the sides, i.e. supposing thermal isolation.

The following section describes a mathematical solution of the heat conduction equation for TE devices, with internal Joule heat generation, and dynamic exchanges of heat through the hot and cold sides.

2. Theory and calculation

In TE devices the Peltier heating or cooling acts only at the junctions where there is the connection with metal, therefore, assuming there are no temperature gradients and losses in the y and z directions, the heat propagation and generation inside the module can be modelled through the one-dimensional, unsteady heat conduction equation with constant thermal conductivity and internal heat generation, expressed as

$$\frac{\partial^2 T}{\partial x^2} + \frac{\dot{g}}{k} = \frac{1}{\varepsilon}\frac{\partial T}{\partial t} \tag{6}$$

where T is the temperature in Kelvin degrees function of both the space x and the time t, $\dot{g}$ is the rate of heat energy generation per unit volume [W/m^3], k is the thermal conductivity coefficient [W/m K], and ε is the thermal diffusivity coefficient defined as

$$\varepsilon = \frac{\text{heat conducted}}{\text{heat stored}} = \frac{k}{\rho C_m} = \left[\frac{m^2}{s}\right] \tag{7}$$

where ρC_m is the heat capacity per unit volume [J/m^3 K].

Our objective is to study TE devices under conditions where both the time and temperatures are varying, hence the temperatures at the hot and cold sides are not considered constant. They are on the contrary considered connected to "far-away" constant temperatures, thus allowing their temperatures to vary depending on the rate of heat flow through them and the generation of heat inside the TE device.

2.1. Description of the problem

To simplify the symmetry of the problem, consider a TE module of thickness 2*L* and area *A*, positioned on the *x*-axis in such a way that the hot side is at $x = -L$ and the cold side at $x = L$. Hence, simplifying the notation, consider the following equation:

$$T_{xx} + \frac{\dot{g}}{k} = \frac{1}{\varepsilon} T_t \tag{8}$$

on the interval $[-L,L]$.

In order to be able to solve this differential differential equation it is necessary to have two boundary conditions and an initial state. The latter is assumed as a linear distribution of temperature throughout the whole module, starting from the initial hot temperature T_{Hi} at $x = -L$, to the initial cold temperature T_{Ci} at $x = L$. Hence the initial condition is

$$T(x,0) = T_0(x) = \frac{T_{\mathrm{Ci}} - T_{\mathrm{Hi}}}{2L} x + \frac{T_{\mathrm{Ci}} + T_{\mathrm{Hi}}}{2} \tag{9}$$

The boundary conditions are those appropriate to the Newton's Law of Cooling, stating that the heat flux (per unit area) out of a boundary with normal n is $q = -kn \cdot \nabla T$, so that the boundary conditions for this problem are written as

$$T_x = \beta_H (T - T_{H\infty}), \quad \text{at } x = -L \tag{10a}$$

$$T_x = -\beta_C (T - T_{C\infty}), \quad \text{at } x = L \tag{10b}$$

where $T_{H\infty}$ and $T_{C\infty}$ are the temperatures "far-away" from the hot and cold sides of the TEG. Fig. 2 illustrates the physical system. β_H and β_C are constants.

2.2. Scaling

It is convenient to appropriately scale the problem in order to identify the important parameter combinations:

$$\begin{aligned} x &= L\xi;\ t = \frac{L^2}{\varepsilon}\tau \\ T &= \Delta T\theta + \frac{T_{H\infty} + T_{C\infty}}{2} \\ \beta_{H,C} &= \frac{\beta_{h,c}}{L};\ \gamma = \frac{\dot{g}L^2}{k\Delta T} \end{aligned} \tag{11}$$

where $\Delta T = (T_{H\infty} - T_{C\infty})/2$. The parameter γ represents how much heat is internally generated by Joule heating compared to the heat flux through the device for conduction, and this is due to the temperature gradient across the device.

After this scaling the problem in Eq. (8) becomes

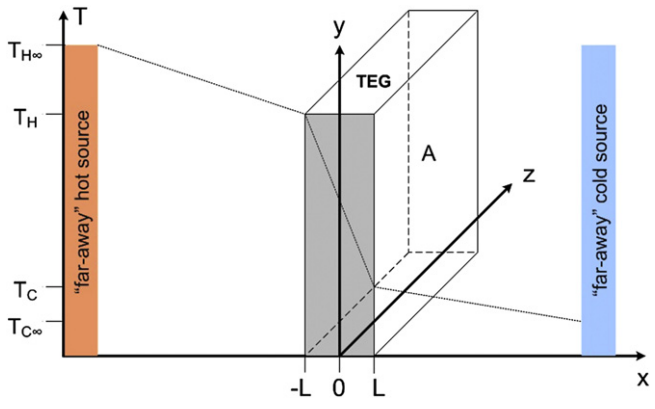

Fig. 2. Physical system considered for the solution of the heat equation.

$$\theta_{\xi\xi} + \gamma = \theta_\tau \tag{12}$$

and the boundary conditions in Eq. (10) become

$$\theta_\xi = \beta_h(\theta - 1), \quad \text{at } \xi = -1 \tag{13a}$$

$$\theta_\xi = -\beta_c(\theta + 1), \quad \text{at } \xi = 1 \tag{13b}$$

Finally, the initial state in Eq. (9) becomes

$$\theta_0(\xi) = \frac{(T_{Ci} - T_{Hi}\xi - (T_{H\infty} + T_{C\infty} - T_{Hi} - T_{Ci}))}{T_{H\infty} - T_{C\infty}} \tag{14}$$

The solution of this problem will be the sum of a steady-state solution and a transient solution, as described in the next two sub-sections. The final solution for θ can then be written as

$$\theta(\xi,\tau) = \theta_{\mathrm{ss}}(\xi) + \hat{\theta}_t(\xi,\tau) \tag{15}$$

where θ_{ss} is the steady-state profile and $\hat{\theta}_t$ is the transient evolution.

2.3. Steady-state solution

We wish to find the steady-state part of the solution in Eq. (15). If $t \to \infty$ then $\partial/\partial t \to 0$, that is $\theta_\tau = 0$. Hence the Poisson's equation $\theta_{\xi\xi} + \gamma = 0$, which leads to

$$\theta_{\mathrm{ss}}(\xi) = A + B\xi - \frac{\gamma}{2}\xi^2 \tag{16}$$

where A and B must be chosen to satisfy the boundary conditions, namely:

$$B + \gamma = \beta_h\left(A - B - \frac{\gamma}{2} - 1\right) \tag{17a}$$

$$B - \gamma = -\beta_c\left(A + B - \frac{\gamma}{2} + 1\right) \tag{17b}$$

leading to

$$A = \frac{\gamma\left(2 + \frac{3}{2}\beta_h + \frac{3}{2}\beta_c + \beta_c\beta_h\right) + \beta_h - \beta_c}{\beta_c + \beta_h + 2\beta_c\beta_h} \tag{18a}$$

$$B = \frac{\gamma(\beta_h - \beta_c) - 2\beta_c\beta_h}{\beta_c + \beta_h + 2\beta_c\beta_h} \tag{18b}$$

2.4. Transient solution

The transient part of Eq. (15), $\hat{\theta}_t$ is

$$\hat{\theta}_{\xi\xi} = \hat{\theta}_\tau \tag{19}$$

with boundary conditions

$$\hat{\theta}_\xi - \beta_h\hat{\theta} = 0 \quad at\ \xi = -1 \tag{20a}$$

$$\hat{\theta}_\xi + \beta_c\hat{\theta} = 0 \quad at\ \xi = 1 \tag{20b}$$

Eq. (19) is the heat equation with homogeneous boundary conditions (Eq. (20)); as such we search for separable solutions and using the transform methods (Fourier transform on finite domain gives Fourier series) we arrive at the following expression for $\hat{\theta}_t$:

$$\hat{\theta}_t(\xi,\tau) = \sum_{\text{allowable } k} (A_k \cos k\xi + B_k \sin k\xi) e^{-k^2\tau} \tag{21}$$

where the coefficients A_k and B_k and the allowable wave-numbers k are determined by the boundary conditions and the initial condition. First we consider the allowable k. The boundary conditions of Eq. (20) give

$$kA_k \sin k + kB_k \cos k - \beta_h (A_k \cos k - B_k \sin k) = 0 \tag{22a}$$

$$-kA_k \sin k + kB_k \cos k + \beta_c (A_k \cos k + B_k \sin k) = 0 \tag{22b}$$

which can be written in matrix form as

$$\begin{bmatrix} \beta_c \cos k - k \sin k & \beta_c \sin k + k \cos k \\ -\beta_h \cos k + k \sin k & \beta_h \sin k + k \cos k \end{bmatrix} \begin{bmatrix} A_k \\ B_k \end{bmatrix} = \begin{bmatrix} 0 \\ 0 \end{bmatrix}$$

whose determinant is

$$|\det| = \left(\beta_c \beta_h - k^2\right) \sin 2k + k(\beta_c + \beta_h) \cos 2k \tag{23}$$

which has non-trivial solutions ($|\det|=0$) for values of k such that

$$\tan 2k = \frac{k(\beta_c + \beta_h)}{k^2 - \beta_c \beta_h} \tag{24}$$

To find a corresponding eigenfunction let's consider Eq. (22a) in the form

$$A_k (k \sin k - \beta_h \cos k) + B_k (k \cos k + \beta_h \sin k) = 0 \tag{25}$$

A corresponding eigenfunction is

$$\psi_k(\xi) = -\beta_c \sin k(\xi - 1) + k \cos k(\xi - 1) \tag{26}$$

Enumerating the solutions of Eq. (24) as k_n, with $0 < k_1 < \cdots < k_n < \cdots$ for $n \in \mathbb{N}$, it can be noted that $tan 2k_n \cong 0$ for big values of k_n. This happens when $2k_n = m\pi$, with m integer, that is when $k_n = m\pi/2$.

The solution for $\hat{\theta}_t$ can then be written as

$$\hat{\theta}_t(\xi,\tau) = \sum_n A'_n \psi_{k_n} e^{-k_n^2 \tau} \tag{27}$$

where the coefficients A'_n are determined by the initial conditions $\theta_0(\xi)$ of Eq. (14), as explained in the following section.

2.5. Transforming the initial condition

The operator defined by $L_k \hat{\theta} = \hat{\theta}_{\xi\xi} + k^2 \hat{\theta} = 0$ with the boundary conditions of Eq. (20) is self-adjoint.

Some notation, let

$$\psi_k(x) = -\beta_c \sin k(\xi - 1) + k \cos k(\xi - 1) \text{ for } k \neq 0$$

and

$$\psi_l^*(x) = \beta_h \sin l(\xi + 1) + l \cos l(\xi + 1)$$

then for $k \neq l$ and both k and l satisfying Eq. (27) we have that

$$\int_{-L}^{L} \psi_l^*(x) \psi_k(x) \mathrm{d}x = 0 \tag{28}$$

and for $k = l \neq 0$ we have that

$$\begin{aligned} \int_{-1}^{1} \psi_k^*(\xi) \psi_k(\xi) \mathrm{d}\xi &= \cos 2k \left[k^2 - \beta_c \beta_h\right] \\ &\quad + \sin 2k \left[\frac{k}{2} + \frac{\beta_c \beta_h}{2k} + \beta_c k + \beta_h k\right] \end{aligned} \tag{29}$$

Suppose the initial condition is $\theta_0(\xi)$, then at $\tau = 0$, we have that $\hat{\theta}_t(\xi, 0) = \theta_0(\xi) - \theta_{ss}(\xi)$. Defining

$$A'_n = \frac{\int_{-1}^{1} \psi_{k_n}^*(\xi)(\theta_0(\xi) - \theta_{ss}(\xi)) \mathrm{d}\xi}{\int_{-1}^{1} \psi_{k_n}^*(\xi) \psi_{k_n}(\xi) \mathrm{d}\xi} \tag{30}$$

Then the solution for θ is

$$\theta(\xi,\tau) = \theta_{ss}(\xi) + n \sum A'_n \psi_{k_n}(\xi) e^{-k_n^2 \tau} \tag{31}$$

The final solution in Eq. (31) obviously needs to be scaled back to temperature using the reverse scaling of Eq. (11).

2.6. The boundary conditions

The boundary conditions used to solve the heat equation come from the Newton's Law of Cooling and they are written in the form of Eq. (10). It is now important to define the coefficient $\beta[\mathrm{m}^{-1}]$ in physical terms.

Considering a body of volume B, with boundaries ∂B, the total energy in the body is

$$E = \int_B \rho C_m T \mathrm{d}V \tag{32}$$

where ρC_m represents the heat storage capability of the body per unit volume [J/m^3 K].

From the heat flux $q = -k \cdot \nabla T$ and the heat conduction equation $\partial T/\partial t = (k/\rho C_m) \nabla^2 T$ comes that the rate of change of energy is

$$\begin{aligned} \frac{\mathrm{d}E}{\mathrm{d}t} &= \int_B \rho C_m \frac{\partial T}{\partial t} \mathrm{d}V = \int_B k \nabla^2 T \mathrm{d}V = \int_{\partial B} k n \cdot \nabla T \mathrm{d}S \\ &= -\int_{\partial B} k\beta (T - T_\infty) \mathrm{d}S = -k\beta A (\overline{T} - T_\infty) \end{aligned} \tag{33}$$

where $\overline{T}$ is the average temperature over the surface ∂B, that is

$$\overline{T} = \frac{1}{A} \int_{\partial B} T \mathrm{d}S \tag{34}$$

Noting the similarity between Eq. (33) and the heat convection equation in the form

$$\dot{q}_{\text{conv}} = -\frac{\mathrm{d}E}{\mathrm{d}t} = -hA(T - T_\infty) \tag{35}$$

where h is the heat convection coefficient [W/m^2 K], it is clear that

$$\beta = \frac{h}{k} = \left[\frac{1}{m}\right] \tag{36}$$

The boundary condition needs to assure continuity of temperature at the two sides of the TEGs. Therefore, depending on if the two sides are in thermal contact with a solid or with a liquid/gas, it

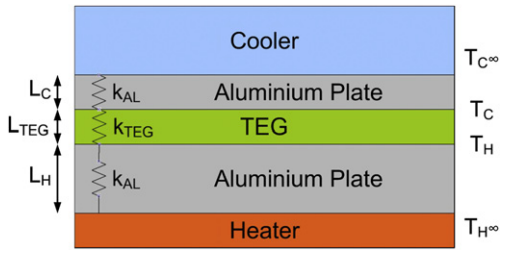

Fig. 3. The system used for all the experiments and simulations (not in scale).

will be necessary to substitute in Eq. (36) the appropriate values, where for a solid h is

$$h_{\text{solid}} = \frac{k_{\text{solid}}}{\text{thickness}} \tag{37}$$

It is preferable to upgrade Eq. (36) to

$$\beta = \frac{h_{\text{medium}}}{k_{\text{TEG}}} = \left[\frac{1}{m}\right] \tag{38}$$

3. Experimental

The solution worked out in the previous section is finally programmed in Matlab, because of the need of a numerical calculator to solve the Fourier series of Eq. (21). Matlab's *symbolic* toolbox has been used.

First, an interval bisection algorithm is used to find the roots of Eq. (24), setting a limit to the maximum value of k. Then for every k the correspondent coefficient A'_n is computed as from Eq. (30) and finally the solution for θ is computed as in Eq. (31) and scaled back to temperature. However this solution does not take into account the electrical behaviour of the TE device (Seebeck effect) and the Peltier effect, which will therefore need to be taken into account in the Matlab model, as described in this section.

Fig. 3 illustrates the system used for all the experiments and simulations in this paper. It is composed by a TEG sandwiched between a heater and a water-cooling block through two Aluminium heat-spreading plates of thickness $L_C = 1$ cm and $L_H = 4$ cm, therefore the h coefficients of Eq. (37) are:

$$h_C = \frac{k_{\text{Al}}}{L_C} = \frac{237\ \text{W/mK}}{0.01\ \text{m}} = 23,700\ \text{W/m}^2\text{K}$$

$$h_H = 5925\ \text{W/m}^2\text{K}$$

The TEG is from Custom Thermoelectric (code: 1261G-7L31-04CQ) and its parameters are:

$$\begin{aligned}&\text{Area} : A = 0.04^2\text{m}^2\\ &\text{Thickness} : L_{\text{TEG}} = 0.004\ \text{m}\\ &\text{Thermal Diffusivity} : \varepsilon \approx 10^{-7}\text{m}^2/\text{s}\\ &\text{Internal Resistance} : R_{\text{int}} \approx 2.5\ \Omega\end{aligned}$$

The thermal diffusivity of Bi_2Te_3 is in the order [13] of 10^{-6}, but the real one is difficult to estimate because of the ceramic layer included in the TEG for isolation and all the interfaces, which slow down the thermal wave, therefore a value of 10^{-7} has been used.

The internal resistance is a function of the average temperature of the module, while the output current and voltage depend on the temperature gradient. Following a similar approach to the one described in a paper by Woo *et al.* [14], the real curves of the electrical characteristic of a TEG can be fitted; in this way, if the temperature gradient ΔT and the load current I_{out} are known, it is possible to mathematically calculate the internal resistance R_{int}, the output voltage V_{out} and the Seebeck coefficient α. For the TEG used:

$$\begin{aligned}R_{\text{int}} &= 0.00531\Delta T + 1.572\\ V_{\text{out}} &= -R^*_{\text{int}} I_{\text{out}} + 0.0453\Delta T - 0.16\end{aligned}$$

$$\alpha = 0.042 + 0.00263\left(1 - e^{-\frac{\Delta T - 50}{50}}\right)$$

Fig. 4 displays both the experimental and the mathematical data for V_{out} versus I_{out} plotted for different values of ΔT. As it can be

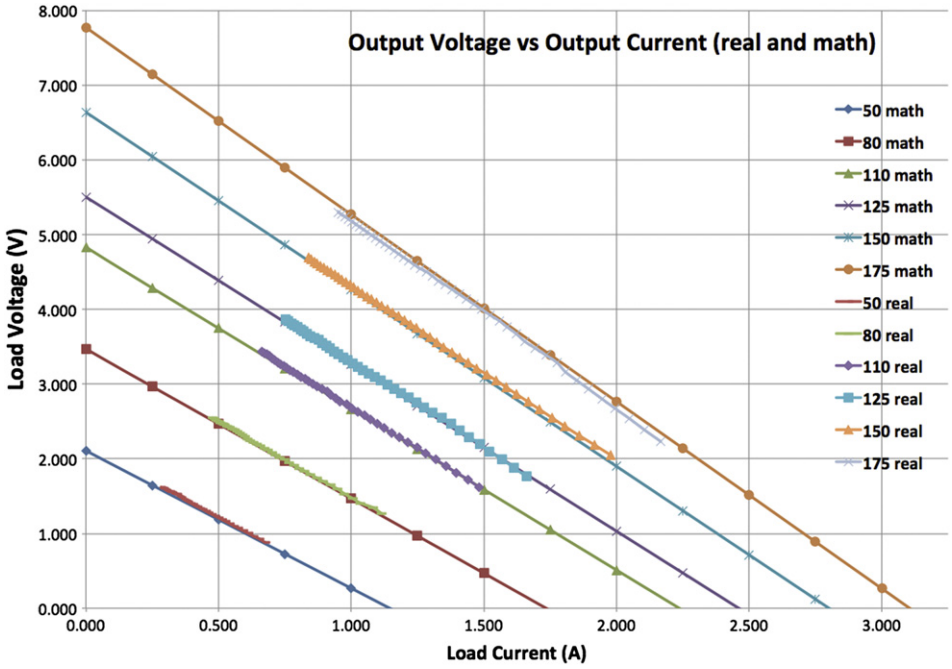

Fig. 4. Experimental and mathematical data for the electrical characterisation of the TEG used, plotted for different values of ΔT.

seen the mathematical functions well approximate the real behaviour of the TEG, hence they can be used in the simulation.

The thermal conduction coefficient of the TEG k_{TEG} has been calculated letting the system get to steady-state with constant input power to the hot side and open-circuit at the TEG terminals:

$$k_{TEG} = \frac{P_{in}A(T_H - T_C)}{L_{TEG}} \approx 1.4\ \mathrm{W/mK} \tag{42}$$

in which the power through the TEG (taking into account the losses of the system), the temperatures at the sides, the area and the thickness are known.

The Peltier effect can be considered a parasitic effect in TE energy generation, because as soon as some current is drawn from the TEG, the Peltier effect brings power from the hot to the cold side, thus increasing the overall thermal conductivity and reducing the temperature gradient (if the heat powers to the hot side and from the cold side remain the same). The Peltier effect is usually greater than the Joule heating effect, therefore it is important to take it into account in the Matlab model. In order to do this, the power from the heater to the TEG through the Aluminium block can be considered as the sum of the Peltier power and the power from $T_{H\infty}$ to T_H in the heat equation. In this way the solution is computed in a loop. At every iteration the heat equation is calculated and the real h coefficient of Eq. (8) (called h_{Hreal}) is modified depending on the Peltier power and called h_{Hmod}:

$$h_{Hmod} = h_{Hreal} - \frac{\alpha T_H I}{A(T_{H\infty} - T_H)} \tag{43}$$

Similar considerations can be applied to the cold side:

$$h_{Cmod} = h_{Creal} - \frac{\alpha T_C I}{A(T_C - T_{C\infty})} \tag{44}$$

Therefore at the end of every iteration β_h and β_c are modified accordingly so that the new steady-state and transient values will account for the Peltier term. The initial condition remains the same.

4. Results and discussion

The solution presented in Section 2 has two main benefits: (1) it allows dynamic exchange of heat power throughout the sides of the TEG and (2) it allows the simulation of transients in TE devices. These features are analyzed in this section.

If the temperatures at the sides were to be assumed constant as in Eq. (3), the effect of Joule heating would be visible only on the points inside the TEG. Fig. 5 shows such a case in a simulation in which the load current is changed. As T_H and T_C are constant, there is no difference in heat transfer through the TEG unless k_{TEG} is modified to account for the change in internal Joule heating.

On the contrary, the steady state solution of Eq. (16) is different because when a load variation takes place T_H and T_C can change even if $T_{H\infty}$ and $T_{C\infty}$ remain constant. In this way it is possible to understand the effect that different loads have on the overall conduction coefficient, i.e. to understand how the temperature gradient across the TEG will change. This can be seen in Fig. 6, and it means that the overall thermal conductivity of the TEG changes.

The effect is more relevant at the hot side because T_H is more distant from $T_{H\infty}$ than T_C is from $T_{C\infty}$. From 0 A to 4 A, T_H decreases

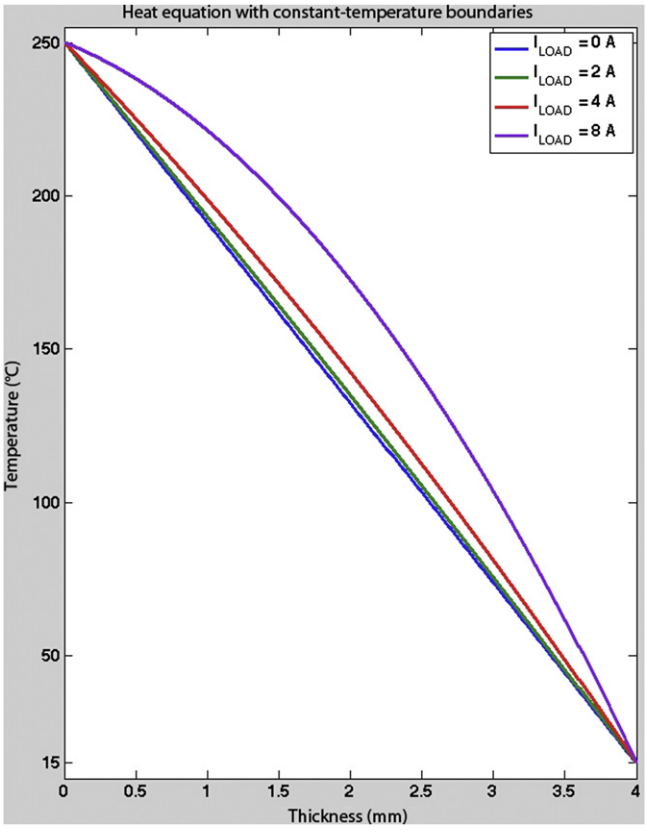

Fig. 5. Heat equation with constant temperature boundary conditions, for different current loads. The hot side is at $x = 0$ mm while the cold side is at $x = 4$ mm. $T_C = 15\ ^\circ C; T_H = 250\ ^\circ C$. Regardless of the load current, the side temperatures are fixed.

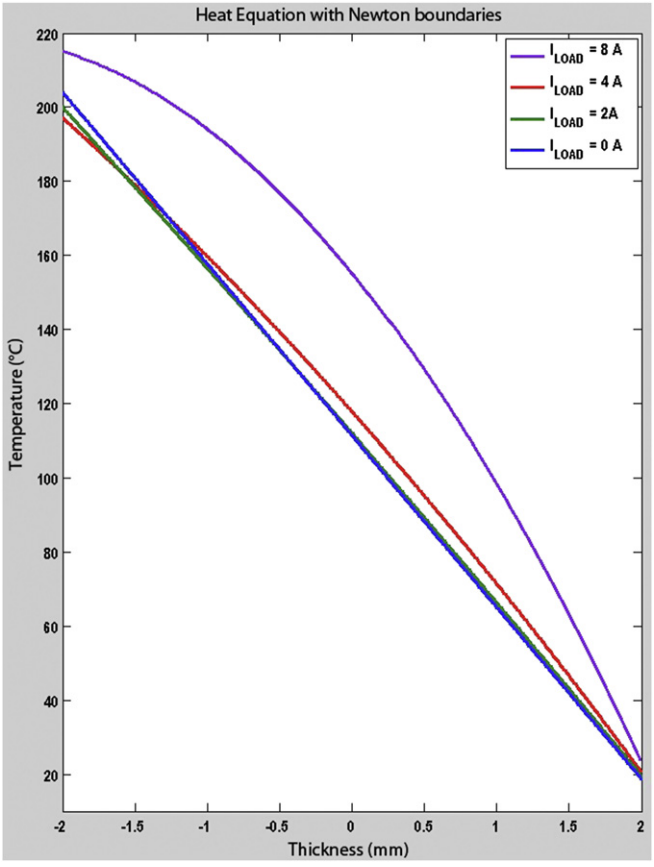

Fig. 6. Heat equation with Newton boundary conditions and Peltier effect, for different loads. The hot side is at $x = -2$ mm while the cold side is at $x = 2$ mm. $T_{C\infty} = 15\ ^\circ C; T_{H\infty} = 250\ ^\circ C$. The hot side temperatures vary with the load current (points: 196, 200, 204.4, 215); the cold side temperatures vary as well (points: 18, 19, 20, 24).

because the Peltier effect is more relevant than the Joule heating, but when the current is 8 A the Joule heating makes T_H increase even more than $T_{H\infty}$; this would suggest an operating point of great efficiency for TEGs, but unfortunately it is not physically possible to make one TEG produce as much current. Anyway it can clearly be understood that the Peltier effect decreases T_H and increases T_C, while the Joule heating increases both T_H and T_C and the temperatures of the other points inside the TEG; this effect depends on the square of the load current, so it becomes quite relevant especially in TE coolers or heaters.

The fact that, when the load current is increased, the term $\alpha T_H I$ of Peltier cooling at the hot side removes more heat than the one brought by Joule heating sets a basilar difficulty in proving with experimental results the heat equation on its own, because there is always the Peltier effect at the interface of the pellets and an ohmic contact; nevertheless, including the Peltier term into the Matlab equation (Eq. (43) and Eq. (44)) and making it run iteratively can provide satisfactory simulations also for real transient experiments.

Steady-state operating points have been compared to the physical system described in Section 3. The system has been brought to steady-state with a load current of 0.1 A, then changed to 1.23 A, always with the same input power to the heater. The comparison is shown in Table 1 and shows that the model can predict T_H and T_C quite accurately.

Fig. 7 simulates the transient from an initial steady-state condition without Joule heating (open-circuit load); at time 0 s the load is suddenly changed to a current of 2.25 A. The plotted curves show the real and simulated transients of T_H and T_C for 23 s. In the experiment, $T_{H\infty}$ is kept at 215 °C with a PID control on the heater, while $T_{C\infty}$ is influenced by a 1 °C hysteresis on the water chiller. During the experiment the cold temperature decreases after a few seconds because the chiller starts cooling down to oppose the change in the water's temperature.

Table 1
Experimental and simulated steady-state operating points. $T_{H\infty}$ and $T_{C\infty}$ of the simulation are set as those of the experiment.

Load	$T_{H\infty}$	T_H	T_C	$T_{C\infty}$
Exp @ 0.1 A	134 °C	125.4 °C	22.9 °C	21 °C
Exp @1.23 A	123 °C	113 °C	23.7 °C	22 °C
Sim @ 0.1 A	134 °C	126.3 °C	22.9 °C	21 °C
Sim @ 1.23 A	123 °C	113.8 °C	23.2 °C	22 °C

It can be seen that the simulation can predict quite accurately the evolution of T_H and T_C during the transient, with an error or around 0.5 °C on T_H.

The solution described by Eq. (31) could be included into a model which takes into account also the thermal masses of the system, thus enabling the possibility of simulating both transients and the final operating point of a complex system. This would constitute a great benefit to the actual engineering task, because when designing a TE system it is difficult to understand what the final operating point will be, because the effects taking place into the TE device will make the temperatures at the side change. In fact $T_{H\infty}$ and $T_{C\infty}$ cannot usually be considered constant. In the case of TE energy generation, the insertion of a TEG changes massively the initially-available hot and cold temperatures, depending on the load and on the capacity of the system to provide and remove hot and cold power. As the solution proposed in this paper analytically dynamically describes what happens inside the TE device, it constitutes the starting point for creating an accurate simulation model.

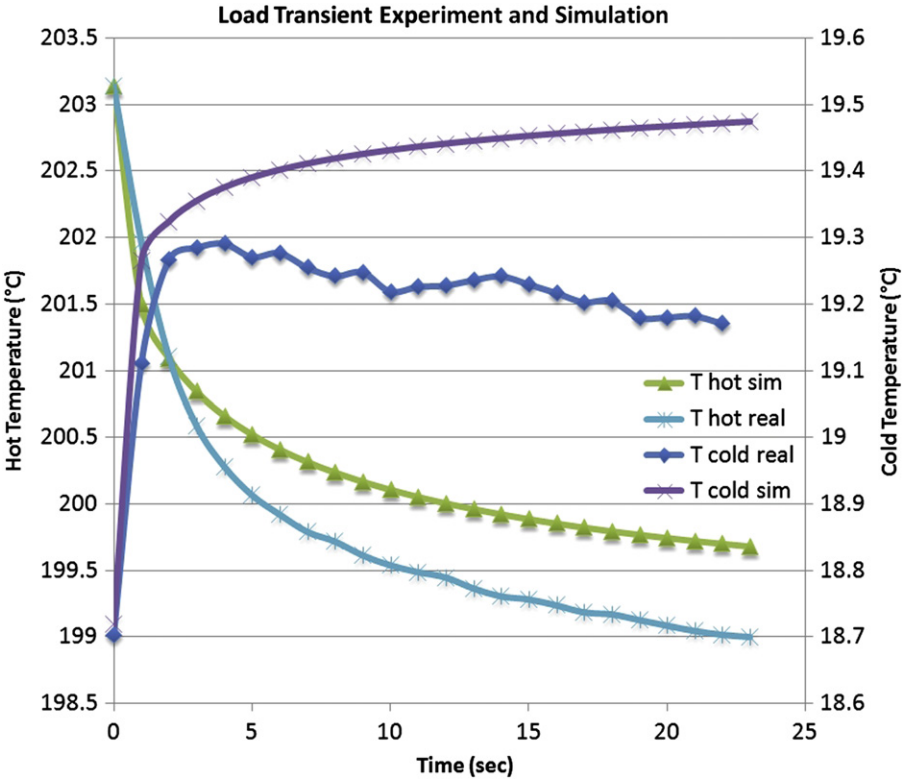

Fig. 7. Load change transient experiment and simulation results. $I_{load} = 0$ *A* @ time = 0 s; $I_{load} = 2.25$ *A* @ time >0 s.

5. Conclusions

This paper provides the solution to the heat conduction equation for TE devices, with internal Joule heat generation, and dynamic exchange of heat through the hot and cold sides. It can be used to study the transient behaviour of TE devices as well as steady-state operation.

The insertion of this solution into a model which describes also the Peltier effect allows the comparison of the simulated results to experimental data, confirming the correctness of the solution.

Future work is adding all the heat masses of the system and the heat and electrical power flow. In this way it would be possible to precisely study transients in TE systems and to work out the final operating point when designing a new system.

Acknowledgements

The authors would like to thank Dr. Steven Roper of the School of Mathematics and Statistics of the University of Glasgow for his great contribution to the project, and the mechanical workshop of the University of Glasgow for their work, creating the test rig used for the experiments.

References

[1] R. Decher, Direct Energy Conversion: Fundamentals of Electric Power Production. Oxford University Press, 1997.
[2] S.W. Angrist, Direct Energy Conversion, third ed. Allyn and Bacon, 1976.
[3] S. Lineykin, S. Ben-Yaakov, Modeling and analysis of thermoelectric modules, IEEE Transactions on Industry Applications 43 (2007) 505–512.
[4] L. Chen, D. Cao, H. Yi, F.Z. Peng, Modeling and power conditioning for thermoelectric generation, 2008 IEEE Power Electronics Specialists Conference (2008) 1098–1103.
[5] M. Chen, L.A. Rosendahl, T.J. Condra, J.K. Pedersen, Numerical modeling of thermoelectric generators with varing material properties in a circuit simulator, IEEE Transactions on Energy Conversion 24 (2009) 112–124.
[6] M. Alata, M.A. Al-Nimr, M. Naji, Transient behavior of a thermoelectric device under the hyperbolic heat conduction model, International Journal of Thermophysics 24 (2003) 1753–1768.
[7] M. Naji, M. Alata, M.A. Al-Nimr, Transient behaviour of a thermoelectric device, proceedings of the institution of mechanical engineers, part A, Journal of Power and Energy 217 (2003) 615–621.
[8] R. E. Simons, R. C. Chu, Application of thermoelectric cooling to electronic equipment: a review and analysis, in: Sixteenth IEEE SEMI-THERM Symposium pp. 1–9.
[9] J. Haidar, J. Ghojel, Waste heat recovery from the exhaust of low-power diesel engine using thermoelectric generators, Proceedings ICT2001 20 International Conference on Thermoelectrics (Cat. No.01TH8589) (2001) 413–418.
[10] J. Yang, Potential applications of thermoelectric waste heat recovery in the automotive industry, ICT 2005. 24th International Conference on Thermoelectrics, 2005 (2005) 170–174.
[11] R. Nuwayhid, A. Shihadeh, N. Ghaddar, Development and testing of a domestic woodstove thermoelectric generator with natural convection cooling, Energy Conversion and Management 46 (2005) 1631–1643.
[12] J.A.B. Vieira, A.M. Mota, Thermoelectric generator using water gas heater energy for battery charging, 2009 IEEE International Conference on Control Applications (2009) 1477–1482.
[13] D.-A. Borca-Tasciuc, G. Chen, A. Prieto, M.S. Martín-González, A. Stacy, T. Sands, M.a. Ryan, J.P. Fleurial, Thermal properties of electrodeposited bismuth telluride nanowires embedded in amorphous alumina, Applied Physics Letters 85 (2004) 6001–6003.
[14] B.C. Woo, D.Y. Lee, H.W. Lee, I.J. Kim, Characteristic of maximum power with temperature difference for thermoelectric generator, 20th International Conference on Thermoelectrics (2001) 431–434.